

Article

Analyses of the Extensible Blade in Improving Wind Energy Production at Sites with Low-Class Wind Resource

Jiale Li ¹  and Xiong (Bill) Yu ^{1,2,*} 

¹ Department of Civil Engineering, Case Western Reserve University, 10900 Euclid Avenue, Bingham Building, Cleveland, OH 44106-7201, USA; jxl780@case.edu

² Department of Electrical Engineering and Computer Science, Case Western Reserve University, Cleveland, OH 44106, USA

* Correspondence: xxy21@case.edu; Tel.: +1-216-368-6247

Received: 24 July 2017; Accepted: 27 August 2017; Published: 30 August 2017

Abstract: This paper describes the feasibility analysis of an innovative, extensible blade technology. The blade aims to significantly improve the energy production of a wind turbine, particularly at locations with unfavorable wind conditions. The innovative ‘smart’ blade will be extended at low wind speed to harvest more wind energy; on the other hand, it will be retracted to its original shape when the wind speed is above the rated wind speed to protect the blade from damages by high wind loads. An established aerodynamic model is implemented in this paper to evaluate and compare the power output of extensible blades versus a baseline conventional blade. The model was first validated with a monitored power production curve based on the wind energy production data of a conventional turbine blade, which is subsequently used to estimate the power production curve of extended blades. The load-on-blade structures are incorporated as the mechanical criteria to design the extension strategies. Wind speed monitoring data at three different onshore and offshore sites around Lake Erie are used to predict the annual wind energy output with different blades. The effects of extension on the dynamic characteristics of blade are analyzed. The results show that the extensive blade significantly increases the annual wind energy production (up to 20% to 30%) with different blade extension strategies. It, therefore, has the potential to significantly boost wind energy production for utility-scale wind turbines located at sites with low-class wind resource.

Keywords: wind turbine blade; extensible blade; smart blade; distributed energy resources; low-class wind resource

1. Introduction

Wind turbines have been used by human beings for more than 3000 years [1]. Its roles have evolved from performing mechanical work such as pumping, grinding and cutting to renewable energy production [2]. Modern wind turbines are typically horizontal axis turbine with two or three blades, which are results of optimal design from both efficiency and cost considerations.

Increasing both the wind power output and efficiency have been consistent goals for the wind energy industry. The proper siting of wind turbines is important to achieve such a goal. It is recommended that wind turbines be constructed at sites with high-quality wind resources. According to TC88-MC 2005 [3], wind resources are classified into four levels depending upon the characteristics of the average wind speed. Many investigations have been conducted into optimizing wind turbine locations for a particular wind farm [4,5]. These include constructing the aerodynamic model to account for the variations of wind flow over hills, ridges, valleys, offshore, and other types of complex topography. However, sites with high-quality wind resources are typically located in remote areas far

away from cities [6,7]. However, more and more wind turbines named ‘distributed energy resources’ are installed at locations with lower-class wind resources [8–10] to take advantages of their close proximity to the existing electrical grid or manufacturing infrastructures. It helps to reduce the development and transportation cost, which offsets to a certain extent the disadvantages of the low-quality wind resource. In contrast to wind farms, which typically contain hundreds of wind turbines, distributed generators are mostly small-scale power generators located close to the service loads. There are a significant number of wind turbines built as distributed energy resources. According to the U.S. Department of Energy’s Distributed Wind Turbine Market Report, 934 MW of distributed wind capacity was installed between 2013 and 2015, representing nearly 75,000 units across 36 states, Puerto Rico, and the U.S. Virgin Islands. Effective utilizing wind resources at sites with low and medium wind speed helps to make wind energy production to be more geographically dispersed; this also helps to reduce the inherent variabilities of wind energy production [11,12].

Improving the energy production at sites with low-class wind bears an important practice value. One potential method is to increase the wind turbine hub height [4,13–16], which utilizes the benefit that the near-ground wind speed increases with elevation. There are, however, significant cost factors associated with manufacturing, logistic transportation, and the construction of components for the higher supporting tower. An alternative method is to develop innovative wind turbine blades technologies that achieve both improvements in production and resiliency. Another alternative method is to develop innovative wind turbine blades that increase both production and resiliency. Significant progress has been made in this aspect. A new design of a dual-rotor wind turbine (DRWT), which includes rotors in both upwind and downwind directions, has been studied by [17]; the authors used the blade element momentum theory to calculate the aerodynamic forces and the torques generated from each of the rotor blades. This dual-rotor wind turbine is considered to have better performance in extracting energy than a conventional single-rotor wind turbine. Huang [18] studied a novel designed wind turbine blade with sinusoidal protuberances with different amplitudes at the leading edge, which was inspired by the structure observed in humpback whale flippers [19]. They used the wind tunnel to test the performance of both the smooth leading edge blade and the comparative models with leading edge protuberances. The results indicated that this new blade has a better performance at the stall region. In Huang and Wu’s study [20], a balloon-type airfoil whose shape changes with the pressure distribution has been introduced. The blade is full of air and is able to change its shape according to the pressure distribution. The authors used the numerical simulation to simulate an NACA0012 airfoil blade and came out with the result that this innovative blade can achieve better aerodynamic performance than the conventional blade. Bhuyan and Biswas [21] described an unsymmetrical cambered airfoil blade for a vertical axis wind turbine (VAWT) which achieves improved performance in self-starting and a high power coefficient. Bottasso [22] investigated a novel passive control concept to mitigate loads and suppress vibrations of wind turbines via a flap or a pitching blade tip that moves passively in response to blade vibrations.

These previous efforts primarily look at dynamically changing the cross-sectional shape of the airfoil in response to wind directions. Meanwhile, the diameter of the rotor is another major factor determining the maximum energy output. Longer blades feature larger sweep areas, and hence capture more kinetic energy. This leads to a lower cost per kilowatt-hour of energy produced, which has been validated by numerous studies [23–27]. According to Jureczko et al. [28], the manufacturing cost of a wind turbine blade is about 15–20% of the total wind turbine production cost. Improving the total power output of a wind turbine via optimizing the wind turbine blades presents an important opportunity to increase the turbine’s cost efficiency.

Besides this, as with most mechanical system, the capacity of the blade should be matched to the wind conditions at a particular site to achieve the best performance. Due to variations in the wind conditions across different sites, it is difficult for a fixed length blade to match the varying characteristics of installation sites. In fact, commercial wind turbine manufacturers supply wind turbines of similarly rated power outputs with different blade lengths for sites with different wind

conditions. A new concept of variable length blade or telescope blade is proposed recently to increase the power output and the annual energy production of the wind turbine [29–31]. The smart blade has an extensible length that will adjust itself according to the incoming wind speed. The blade will extend at low wind speeds to harvest more wind energy, and it will retract to its original shape when the wind speed is above the ‘rated wind speed’ to ensure structural safety. Therefore, it will produce more energy while protecting the blade from possible damage under high wind speeds. Although this variable length blade has been proposed for several years, there is very limited information on the aerodynamic performance characteristics of this blade. In addition, the blade concepts in previous studies are only extended at the blade tip.

This paper analyzes the concept of the smart blade with the extensible length adjusted according to the incoming wind speed. The blade will extend at low wind speeds to harvest more wind energy and it will retract to its original shape when the wind speed is above the ‘rated wind speed’ to ensure structural safety. Therefore, it will provide more wind energy outputs while protecting the blade from possible damage under high wind speed. The performance of this extensible blade was analyzed using blade element momentum (BEM) theory, which is an accepted method by the wind industry for wind turbine blade aerodynamic calculation and therefore provides practice feasible conclusions. The BEM model is firstly validated with the field-monitored energy production data of regular wind turbines. The performance of the extensible blade is then analyzed using field-monitored wind speed data at a few onshore and offshore sites around Lake Erie. The results show the promise of the extensible blade to significantly improve energy production at sites with a low class of wind resources.

2. Extensible Blade Concept

The theoretical power output of a wind turbine is described in Equation (1) [32,33].

$$P = \frac{1}{2} C_p \rho A U_{\text{tot}}^3 \quad (1)$$

where ρ is the density of air, C_p is the power coefficient, A is the rotor swept area, and U_{tot} is the inflow wind speed.

The equation shows that, at a certain inflow wind speed and air density (which are primarily decided by the climate condition and the topology of a particular site), the power output of a wind turbine is dependent upon its power coefficient and the rotor swept area. The power coefficient is decided by the mechanical structure of the rotor, with the theoretical maximum given by the Benz limit. The rotor swept area is decided by the length of the blade. The blade length is typically controlled from safety consideration to prevent the structural failure at a critical high wind speed which is rarely exceeded in the turbine service life. In this sense, the fixed length blade is not optimized to work under low wind speed conditions. The low wind speed allows the blade length to be increased to improve the wind turbine production while posing no threat to its structure safety.

The basic idea of the extensible blade is to increase the blade length at lower wind speed to produce more energy; the blade will turn to its original length when the inflow wind speed exceeds the rated wind speed. Therefore, an improved power output curve will be achieved for all the working conditions while mitigating safety risk. To study the technical feasibility without losing generality, two types of blade extension scenery are analyzed to assess the benefits of the extensible blade in wind energy production; i.e., (1) extension at the middle of the blade and (2) extension at the tip of the blade (Figure 1). In these analyses, the extensible part of the blades is assumed to have the same foil size as the connection parts. The parameters of the prototype turbine blade are first determined. Aerodynamics analyses are conducted on the extensible blade at different extension conditions. The performance of the extensible blade in energy produced is compared with regular blade using the wind speed data at three different sites in Lake Erie area, Cleveland, LA, USA.

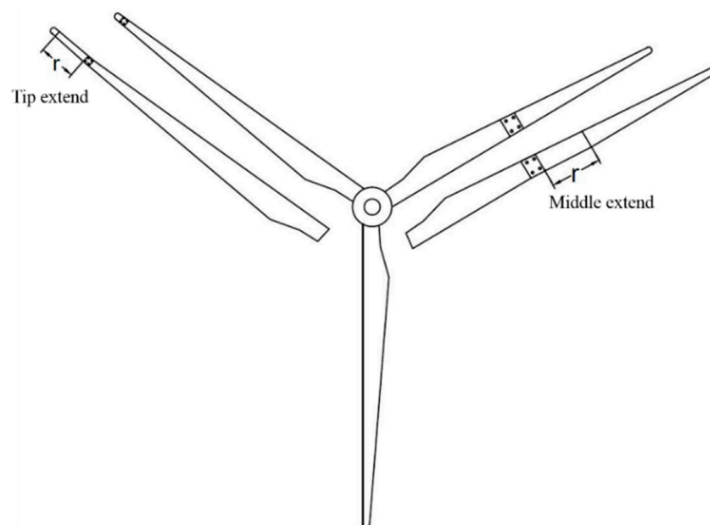


Figure 1. Schematic of the extensible blade concept (with an illustration of extension at the tip and middle of the blade).

3. Specifications of Fixed Length Wind Turbine Blade

The baseline turbine model is built based on a 100 kW utility-scale wind turbine (Northern Power[®] 100, Northern Power Systems, Barre, VT, USA), installed on the campus of Case Western Reserve University. The key parameters of the turbine are shown in Table 1. The manufacturer power curve is plotted in Figure 2. The turbine was installed in November 2010 with financial support from the Ohio Third Frontier Program. The primary role of the turbine is to serve as a research test-bed for wind energy research [34]. A Campbell-Scientific data acquisition system (DAQ) is installed in the wind turbine tower to monitor the operation data, i.e., wind speed, wind direction, output power, etc. continuously.

Table 1. Prototype wind turbine parameter.

Configuration	Description
Model	Northern Power [®] 100
Design Class	IEC IIA
Design Life	20 years
Hub Heights	37 m
Power Regulation	Variable speed, stall control
Rotor Diameter	21 m
Rated Wind Speed	14.5 m/s
Rated Electrical Power	100 kW, 3 phase, 480 VAC, 60/50 Hz
Cut-In Wind Speed	3.5 m/s
Cut-Out Wind Speed	25 m/s

Wind energy is produced due to the lift force on the blade produced by the incoming air flow, which drives the rotor. The airfoil shape characteristics are the essential factors determining the lift force. The model used in this research is based upon the airfoil DU-00-W-401 from the well-known NREL 5-MW prototype wind turbine. Because the blade profile data is unavailable for the 100 kW prototype wind turbine, the model used in this research is based upon the airfoil DU-00-W-401 from the well-known NREL 5-MW prototype wind turbine [35] and scaled down to the length of a 100 kW turbine. The detailed profile data of the 5-MW prototype wind turbine is available for research purposes. The lift and the drag coefficient of DU-00-W-401 are plotted in Figure 3. As a simplification, the airfoil is assumed to have the same shape from root to tip of the blade, with a decreasing chord length. The chord length of a blade is defined as the width of the wind turbine blade at a given distance

along the length of the blade (Figure 4). In this study, the rotor shape of the NREL 5-MW reference wind turbine is scaled down to the 21 m diameter blade with the corresponding chord lengths scaled and shown in Table 2.

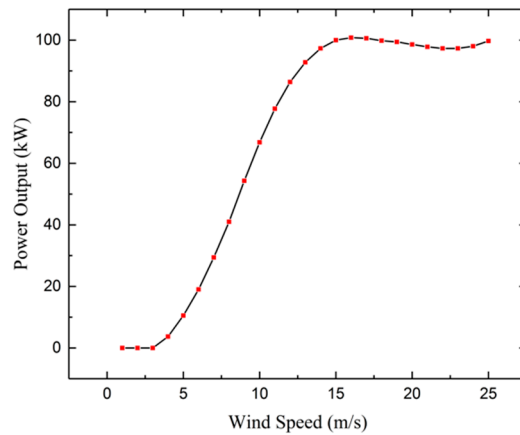


Figure 2. Power curve of the 100 kW wind turbine.

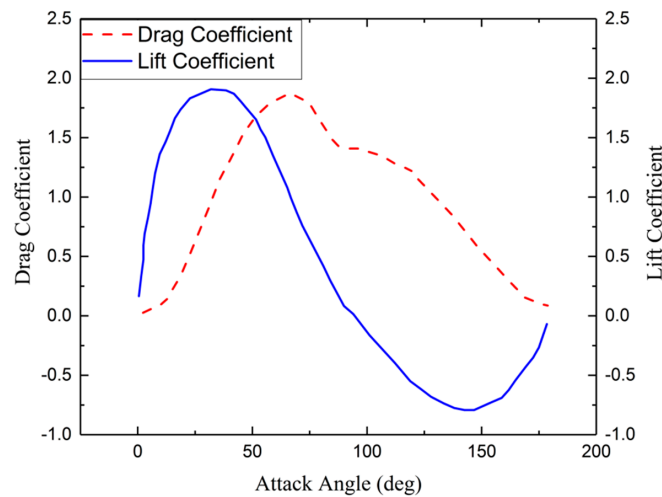


Figure 3. DU-00-W-401 airfoil lift and drag coefficients [35].

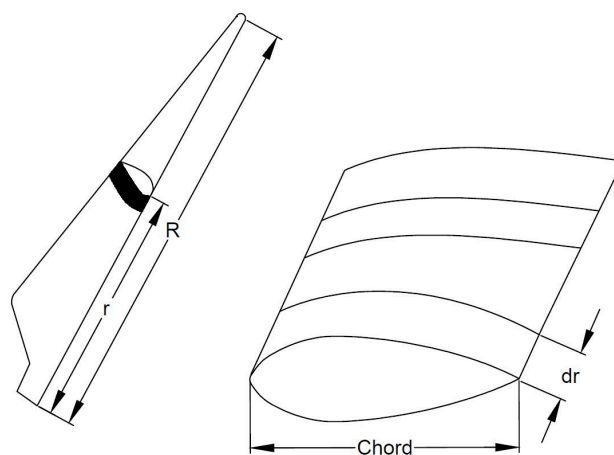


Figure 4. Schematic of the blade with an example airfoil blade element (r is the distance from blade’s root to airfoil blade element, R is the blade radius, and the chord length is that of the straight line joining the leading and trailing edges of an airfoil).

Table 2. Parameters for each section along the blade based on 5 MW prototype wind turbine scaling to blade length of 10.52 m [35].

Radius (m)	Twist (Deg)	Chord (m)	Airfoil Shape
0.48	13.31	0.59	Cylinder
0.93	13.31	0.64	Cylinder
1.39	13.31	0.69	Cylinder
1.96	13.31	0.76	DU-00-W-401 ^a
2.65	11.48	0.78	DU-00-W-350
3.33	10.16	0.74	DU-00-W-350
4.02	9.01	0.71	DU-97-W-300
4.70	7.79	0.67	DU-91-W2-250
5.39	6.54	0.63	DU-91-W2-250
6.07	5.36	0.58	DU-93-W-210
6.76	4.19	0.54	DU-93-W-210
7.44	3.13	0.50	NACA64618 ^b
8.13	2.32	0.46	NACA64618
8.81	1.52	0.42	NACA64618
9.38	0.86	0.38	NACA64618
9.84	0.37	0.35	NACA64618
10.29	0.11	0.24	NACA64618
10.52	0	0.15	NACA64618

^a DU stands for Delft University; ^b NACA stands for National Advisory Committee for Aeronautics.

4. Model and Analyses of the Original Length Blade and Extensible Blade

The aerodynamic analyses are conducted on the original fixed blade as well as the extensible blades using the blade element momentum (BEM) theory. BEM theory is a classical analysis method of wind turbines [36], which has been widely accepted for blade performance analyses; an established model such as BEM is selected for these analyses so that the results provide a practical assessment of the new blade technology. BEM is composed of two different theories; i.e., blade element theory and momentum theory [37]. Blade element theory assumes that blades can be divided into small elements that act independently of the surrounding elements and operate aerodynamically as two-dimensional airfoils as shown in Figure A1, in which α is the attack angle. The characteristics of blade responses (drag and lift on each element) are determined by the angle of attack of incoming wind, which is the angle between the center reference line of the geometry and the relative incoming flow W (Figure A1). The momentum theory assumes that the loss of air pressure or the generation of turning momentum in the airfoil blade element is caused by the work done by the incoming airflow [38]. The BEM theory couples these two theories together and calculates the total lift and momentum via an iterative process [39]. The model is subsequently used to determine the power output at a given wind speed.

The BEM theory is implemented via customized code developed with MATHCAD® (MATHCAD 15.0, Parametric Technology Corporation, Needham, MA, USA). Details of the implementation procedures for the BEM theory are provided in the Appendix A as they are not the focus of this paper.

Validation of BEM Model in Blade Power Output Prediction

For implementing the BEM model analyses, the 10.5 m prototype blade is divided into 30 sections each with a width of 0.35 m. The number of section and the section width are determined based on the results of a sensitivity study, which achieves computational efficiencies while ensures the accuracy.

The performance of the developed BEM model in power output prediction is firstly validated by utilizing the monitored power production data from the 100 kW utility-scale wind turbine described in Section 3. The data is collected at 10 min time interval between September 2014 and August 2015, which includes the air density, the rotational speed of the blade, the wind speed at hub height, and the power output. Measured wind speed, blade rotational speed, and air density are used to calculate the power output using the described BEM model. The monitored power outputs at different wind speeds

are compared with those predicted by the BEM model in Figure 5. Also shown in this figure are the curve fitting of the measured or BEM model predicted power output. In general, the predicted power output performance matches well with the measured data. The monitored total energy output during the one-year period is 388.87 MWh, while the energy production predicted by the BEM model is 397.52 MWh. For wind speeds under 6 m/s, the curve fitted turbine power curve from the BEM model prediction is slightly beneath that from the monitoring power production data; the trend reverses for wind speeds larger than 12 m/s. One of the causes is the limited amount of data available at high wind speed range. Overall, the maximum error between the BEM model's predicted output and monitored data is within 2.2%. The comparison with the monitored wind turbine power output data validated that the BEM model is accurate in predicting the wind energy output. Subsequently, the validated BEM model was utilized to analyze the performance of the proposed extensible blade in the subsequent section.

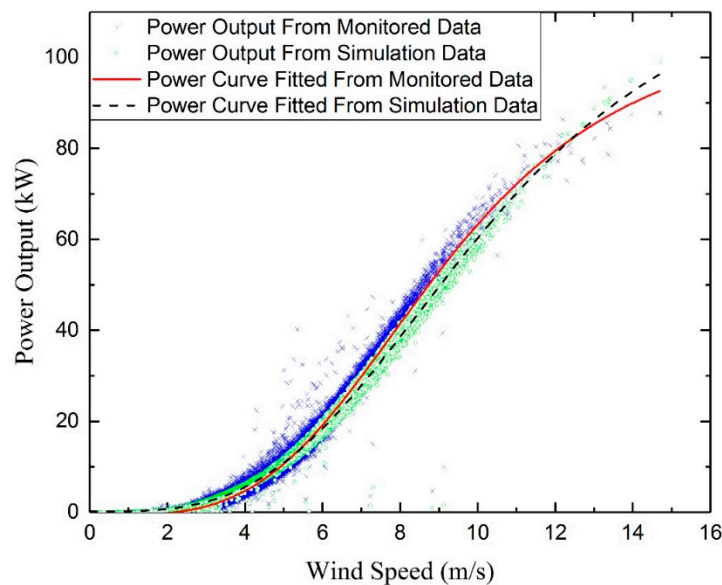


Figure 5. Comparison of the blade element momentum (BEM) model's predicted power output and the monitoring power output of the 100 kW wind turbine.

5. Analyses of Extensible Blade Performance with the BEM Model

5.1. Wind Characteristics at Studied Sites

A few utility scale wind turbines have been erected as part of the efforts of the State of Ohio in promoting renewable wind energy both onshore and offshore [6,40–42]. These wind turbines serve as the case studies in this research. According to the National Oceanic and Atmospheric Administration (NOAA), the monthly average wind speed in Cleveland is 4.69 m/s, or Class 4 according to TC88-MC 2005. Winter is the windiest season in Cleveland with average wind speeds reaching 5.36 m/s, or on average 28% higher than wind speeds in the other seasons. On the other hand, summer features the lowest average wind speed of 3.93 m/s. This pattern of seasonal wind speed is consistent with the seasonality pressure gradients across Cleveland and the Great Lakes region [43]. Three instrumented locations with different typical wind resources are selected to evaluate the potential performance of the extensible blade, including two locations onshore and one location offshore (Figure 6).

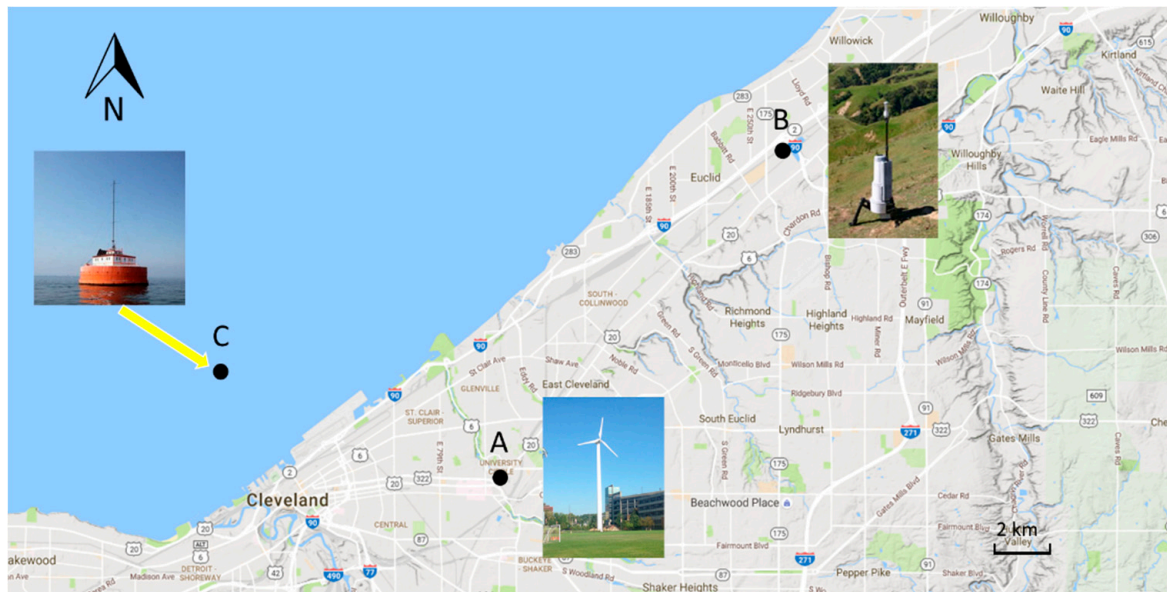


Figure 6. Location of selected sites with wind condition measurement.

For all these sites, the data of wind conditions have been monitored over the years (2006–2015). The data set include wind data at 10 min time interval at the three locations as shown in Figure 6, i.e., site A (on the campus of Case Western Reserve University (CWRU)); site B (along an interstate highway and adjacent to manufacturing facility); and site C (offshore Lake Erie). The data for location A is provided by the data acquisition system (DAQ) installed in the 100 kW wind turbine on CWRU campus. The data for location B is from Lidar measurement of the wind speed. Data from location C is from the met mast, which is installed on a water intake crib 5 miles offshore of Lake Erie.

5.2. Weibull Distribution

Weibull distribution is the most widely used probability distribution to present wind data. The general form of the Weibull density function is a two parameter function, which is given as [44]:

$$f(U_{\text{tot}}) = \frac{k}{c} \left(\frac{U_{\text{tot}}}{c} \right)^{k-1} e^{-(U_{\text{tot}}/c)^k} \quad (2)$$

where $f(U_{\text{tot}})$ is the probability density function, also referred to as PDF; U_{tot} is the wind speed (m/s); c is the scale factor (m/s), and k is the shape factor. The maximum likelihood method (MLM) is used in this research to calculate the Weibull scale and shape factors according to our 10 min time intervals of data availability [45]. The shape factor and scale factor could be calculated as follows [46,47]:

$$k = \left(\frac{\sum_{i=1}^N U_i^k \ln(U_i)}{\sum_{i=1}^N U_i^k} - \frac{\sum_{i=1}^N \ln(U_i)}{N} \right)^{-1} \quad (3)$$

$$c = \left(\frac{1}{N} \sum_{i=1}^N U_i^k \right)^{1/k} \quad (4)$$

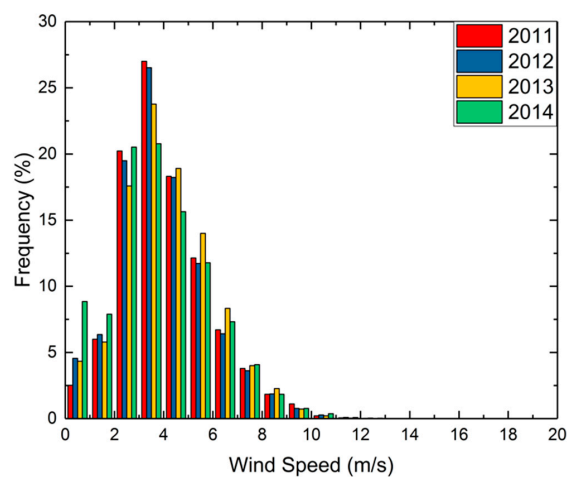
where U_i is the average wind speed in time step i and N is the total number of nonzero wind speed data points.

5.3. Adjustment of Wind Speeds with Elevation

The wind speed data collected by Lidar system at site B and met mast at site C are both measured at the height of 30 m above the ground, and the prototype wind turbine has a hub height of 37.5 m. Therefore, the wind speed is adjusted to the hub height of the prototype wind turbine. The most common method to adjust the wind speed over different height is the power law model, where the wind speed at any height above the ground can be determined using the following expression [48]:

$$U_z(z) = U_{\text{ref}} \left(\frac{z}{z_{\text{ref}}} \right)^{\alpha_0} \quad (5)$$

where z is the target height, z_{ref} is the reference height above the ground [49], and the U_{ref} is the reference wind velocity measured at reference height. The exponent, α_0 , will change with the terrain roughness and the surrounding building height range, which also refers as the wind shear coefficient (WSC). The WSC in the above equation depends on the terrain type from very flat terrain to dense urban, and its value at different terrain types can be referred to previous studies [50]. The WSC value for site B is chosen as 1/4, which is the suggested value for the rural area; the WSC for site C is chosen as 1/9, which is the suggested value for the water surface. The measured wind speed data at site B and site C are adjusted from 30 m to 37.5 m from Equation (5). The wind speed distribution at 37.5 m height in a typical year is shown in Figure 7 for each of the three sites. It can be concluded from Figure 7 that the wind speed distribution at the same location has slightly bias in different years, but the overall trend is similar. The wind speed at site A is more concentrated with the highest frequency at 4 m/s, and the wind speed at site C is more distributed, varying from 0 m/s to 25 m/s. The statistical characteristics of the wind speed data for these three locations are summarized in Table 3. Overall, site A has the lowest mean wind speed since the site is surrounded by a few buildings with heights of up to 20 m. The wind speed of site B is slightly higher because the site is located in a rural area that most of the surrounding buildings are under 10 m in height. The offshore site C has the strongest wind speed since the terrain is flatter at the offshore location. Both Sites A and B are classified as Class 4 while Site C barely qualifies as Class 3 wind site according to IEC standard [3].



(a)

Figure 7. Cont.

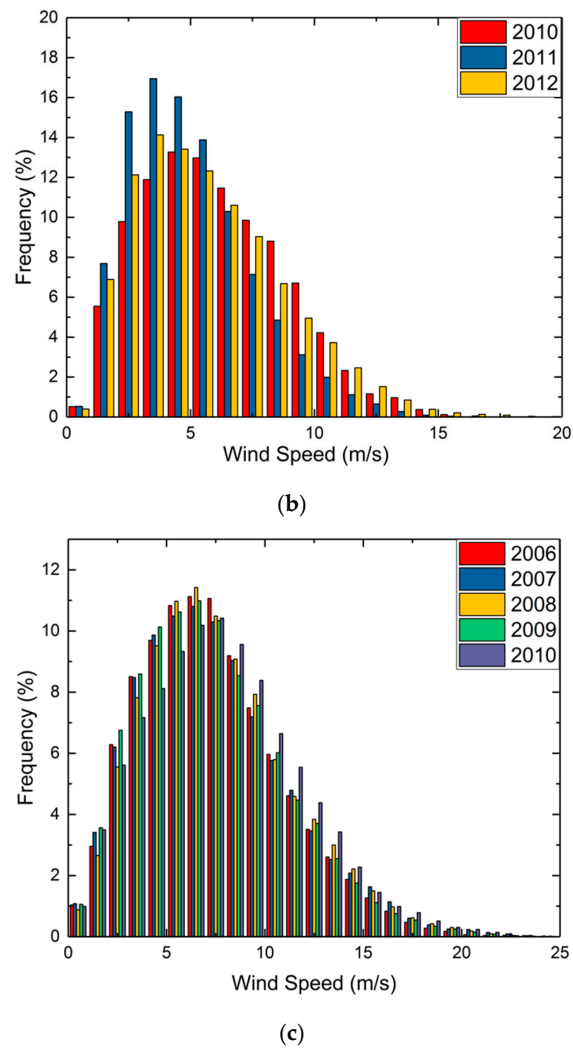


Figure 7. Weibull distribution of wind speed data at 10 min intervals at (a) Site A; (b) Site B; (c) Site C.

Table 3. Locations and mean wind speed characteristics.

Location	Year	Mean Wind Speed (m/s)	S.D. (m/s)	Weibull Shape Factor k	Weibull Scale Factor c (m/s)	Note
Site A 41°30'08.6'' N 81°36'19.9'' W (IEC Class 4)	2011	4.01	SD = 1.797	2.26	4.53	NA
	2012	3.96	SD = 1.05	2.00	4.37	NA
	2013	3.95	SD = 0.69	2.30	4.65	NA
	2014	3.80	SD = 1.52	1.48	4.07	NA
Site B 41°36'07.8'' N 81°29'48.7'' W (IEC Class 4)	2010	5.99	SD = 2.84	2.25	6.78	October to December
	2011	4.98	SD = 2.49	2.13	5.64	April to December
	2012	5.71	SD = 2.96	2.05	6.46	January to April
Site C 41°32'53.7'' N 81°44'58.7'' W (IEC Class 3)	2006	7.35	SD = 3.64	2.13	8.31	NA
	2007	7.46	SD = 3.85	2.04	8.43	NA
	2008	7.62	SD = 3.78	2.12	8.61	NA
	2009	7.29	SD = 3.73	2.06	8.24	NA
	2010	7.82	SD = 3.87	2.13	8.83	NA

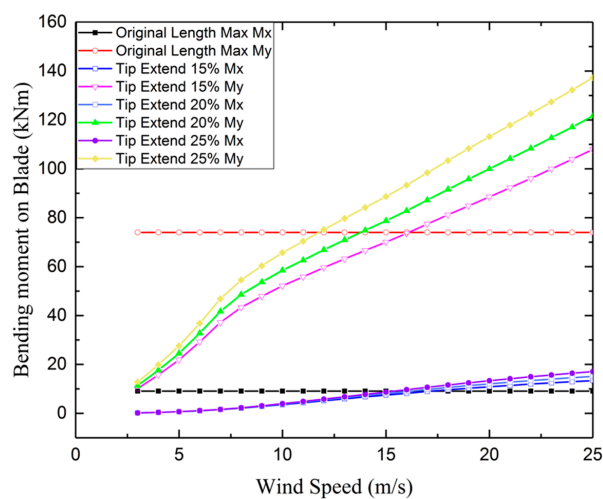
5.4. Analyze the Energy Production Performance of the Extensive Blade

5.4.1. Determination of the Working Range of Wind Speed for Extensible Blades

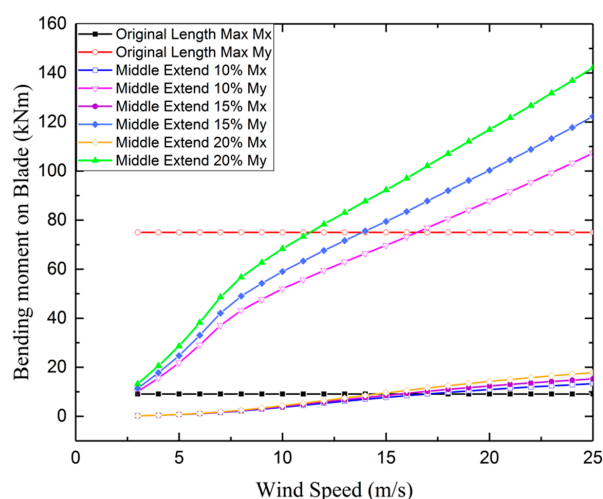
The extended blade is subjected to a higher wind load. Therefore, determining the range of working wind speed is firstly conducted to ensure the safety of the blade. Since the focus of this

study is to assess the feasibility of the extensible blade for improving energy production, simplified mechanical analyses are conducted rather than sophisticated evaluations. The maximum allowed working wind speed is determined based on the corresponding bending moment on the extended blade, whose value should not exceed the bending moment of the original length blade at the cut-out wind speed [51].

With these criteria, the ranges of working wind speeds for two types of extensible blades are analyzed; i.e., (1) different extent of extension at blade tip; and (2) the different extent of extension in the middle of the blade. By using the BEM model, maximal in-plane and out-of-plane bending moments in the original blade and extended blades at different wind speeds are shown in Figure 8, and the intersection points are limits that determine the range of operational wind speed for the extensible blade. Ranges of safe working wind speeds corresponding to the different extension of the blade are determined, which are summarized in Table 4. As a note, from an operation perspective, the scheme of extension is designed to be simple (i.e., extension at steps of 25%, 20%, 0%) so that blade extension is not too frequent to conserve the energy needed for blade actuation. More sophisticated extension schema can be designed based on further analyses of wind characteristics.



(a)



(b)

Figure 8. (a) Determination of the wind speed range for (a) blade extension at tip and (b) blade extension in the middle.

Table 4. Blade extends type in the research.

Extension Method	Wind Speed Range (m/s)	Extension (%)
Extensible blade with tip extension	3–10	25
	10–14	20
	14+	0
Extensible blade with middle extension	3–10	20
	10–14	10
	14+	0

5.4.2. Modal Analysis

A modal analysis determines the vibration characteristics (natural frequencies and mode shapes) of a structure. The natural frequencies and mode shapes are important parameters affecting the response and design of a structure for dynamic loading conditions. A good design for reducing vibration is to separate the natural frequencies of the structure from the harmonics of rotor speed [52]. The modal analysis of the extensible blade helps us understand how the natural frequencies change, thus avoid resonance when the large amplitudes of vibration could damage the wind turbine.

The FEM software COMSOL[®] (COMSOL 5.0, COMSOL, Inc., Burlington, MA, USA) is used to calculate the un-damped modal characteristics of the turbine. The wind turbine blade is considered as a cantilever beam with blade root fixed. The program solves the following eigenvalue problem [53] utilizing the model's stiffness and mass matrices.

$$[K - \omega^2 M]\{\phi\} = \{0\} \quad (6)$$

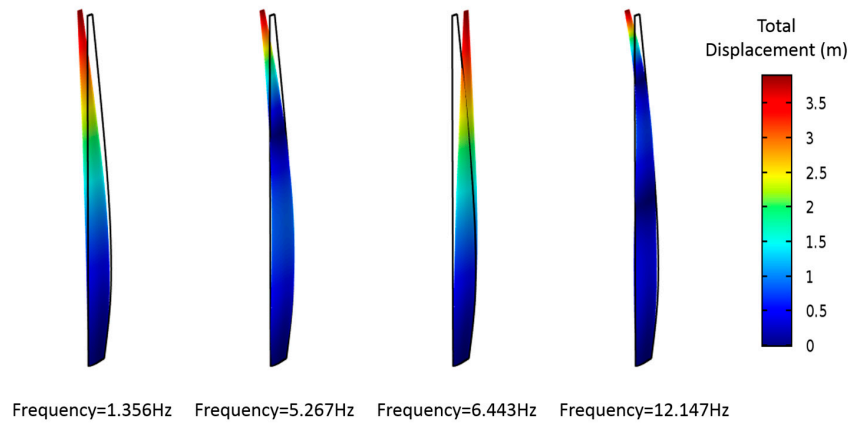
Equation (6) is a typical real eigenvalue problem; therefore, ϕ has a non-zero solution if the value of its determinant coefficient is zero.

Typically, only the first few natural modes are of interest for structural engineering design as they typically contain most of the modal mass and have natural frequencies close to the excitation frequency of the wind. In this research, only the first four natural frequencies are considered; as the finite element model considered here is a simplification of the structure intended to capture global structural dynamic demands, the higher mode results will likely be less accurate. For comparison purposes, both the tip-extend and middle-extend strategy are extensions of 20% of its length.

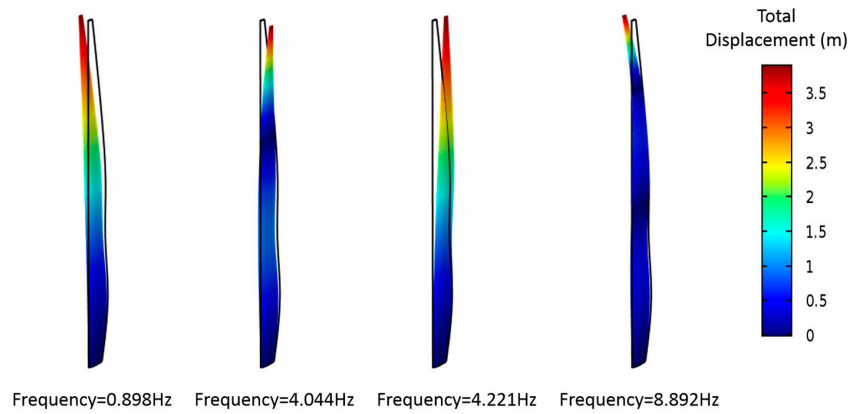
Table 5 presents the results of modal analysis with the first four modes. Overall, increasing the length of the blades reduces its natural frequencies. From the results of the modal analysis, the dominant vibration mode for the horizontal across wind direction has a natural frequency of 1.356 Hz for original length blade, 0.8982 Hz for middle extend 20% blade and 1.104 Hz for tip extend 20%. The natural vibration mode shapes are shown in Figure 9.

Table 5. Modal Frequency.

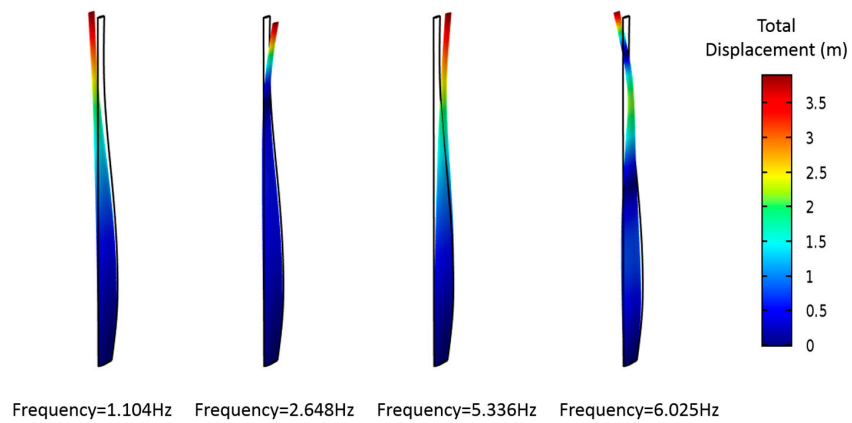
Model Shape	Original Length (Hz)	Middle Extend 20% (Hz)	Tip Extend 20% (Hz)
1	1.3562	0.8982	1.104
2	5.2671	4.0438	2.6484
3	6.4427	4.2213	5.3358
4	12.147	8.8918	6.0251



(a)



(b)



(c)

Figure 9. The shapes of first four modes for (a) original length blade; (b) blade-extension of 20% at the tip; (c) blade extension of 20% in the middle.

5.4.3. Performance of Extensible Blade in Wind Energy Production

With the extension strategy defined by base structural safety considerations, which are summarized in Table 3, Figure 10 compares the corresponding power output curves of the extensible blades with that of the original blade. Both the manufacturer's power curve and the power curve from a curve fitting of the monitoring data are plotted for comparison purposes. It is noted that the power curve from the monitoring data does not cover a high wind speed range. The predicted power curves of the extensible blade by the BEM model with two different extension strategies are also plotted. The comparison clearly shows that the extended blade has a much higher power output at wind speeds lower than the blade's rated wind speed of 14 m/s. There are different extents of shift in the power production curves at wind speed of 10 m/s is due to the proposed blade extension strategy that changes the extent of blade extension at 10 m/s (Table 4). It is assumed that the maximum output is limited to 100 kW to match the capacity of the generator (modified power curve shown in Figure 10). It can be seen from the figure that the power curve from the BEM model and the power curve from the monitored data are closer to each other but different from the manufacturer's power curve. This is because the manufacturer's power curve is measured under certain meteorology conditions which are different to the real conditions [54]. The blade production curves of extensible blades are similar to the original blade as they are completely retracted to the original length. Since the wind speed at the three selected sites was under 14 m/s for most of the time (Figure 7), it is expected that a turbine with extensible blades will consistently produce more energy than a regular turbine for the majority of the year. The annual energy output of the extensible and original length blade can be calculated using the corresponding power curves and the wind speed data at the three test sites.

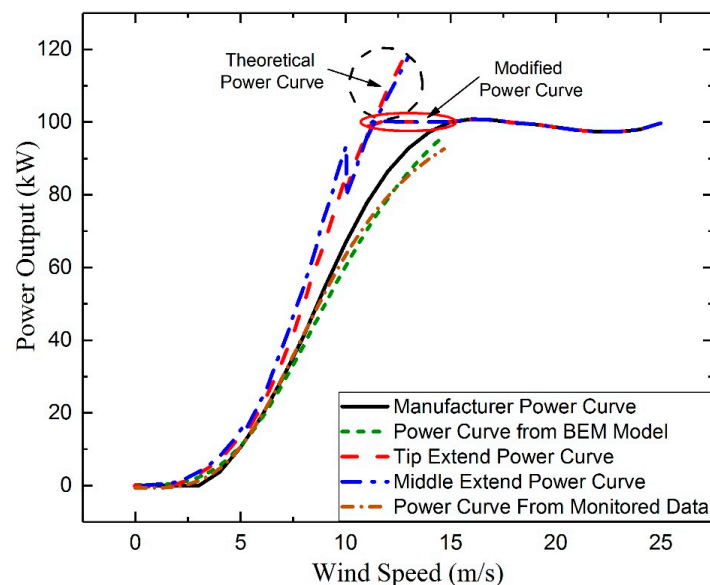
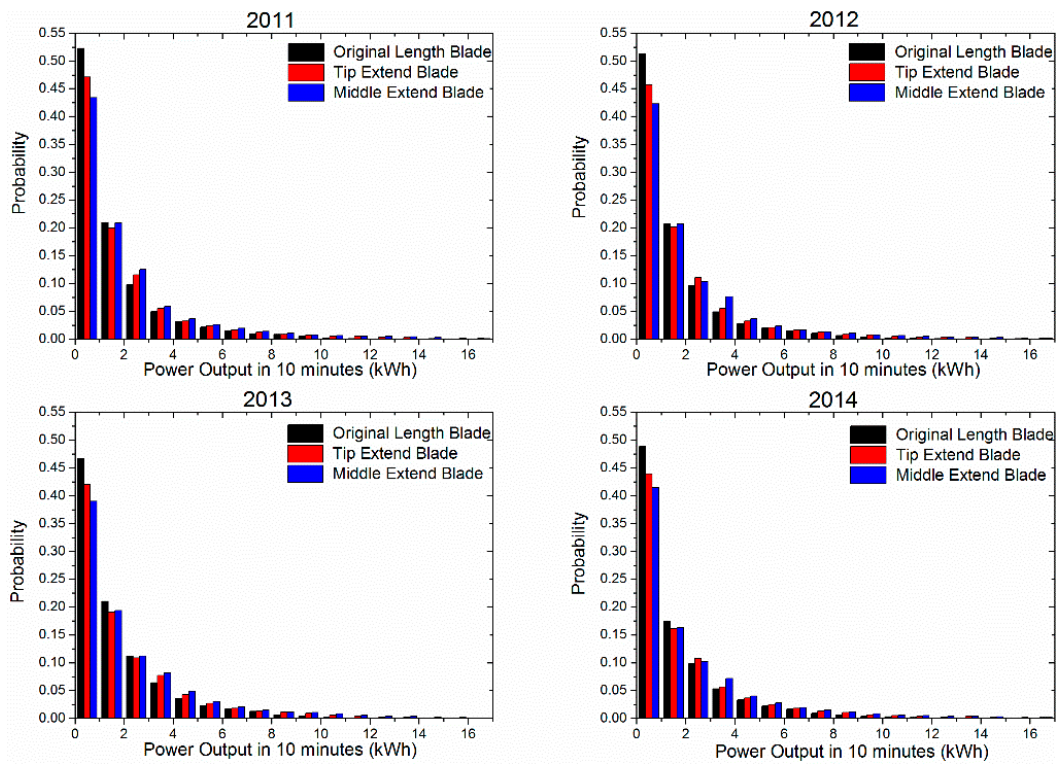
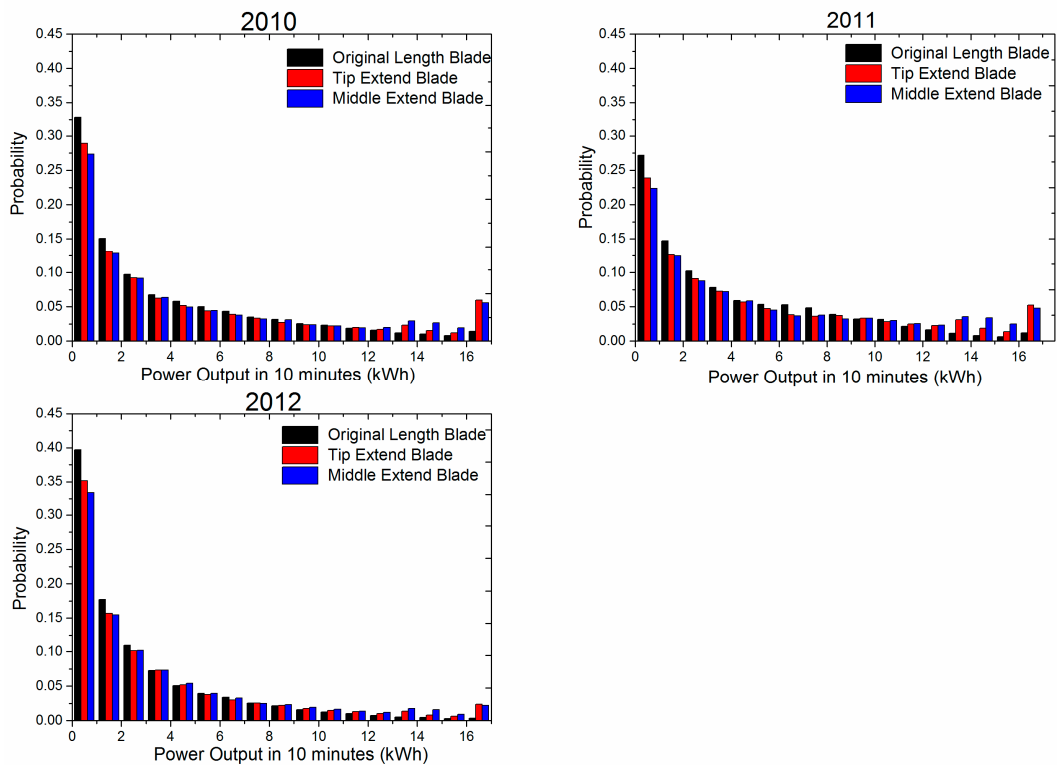


Figure 10. Comparison of the power curves for the original length blade, tip-extended blade and middle-extended blade.

The monitored yearly wind speed data at the three locations with the low-class wind (A and B: Class 4 and C: Class 3) are utilized to estimate the total wind energy outputs, following the validated procedures described in the earlier context. Figure 11 shows the histogram of the predicted average power output in 10 min intervals for each site for different years with the baseline blade and extensible blades. Overall, the comparison shows that the original baseline blade has a higher occurrence of low-energy output periods than the extended blades. In another word, the extensible blades shift the wind energy production to higher energy output than an original blade for these sites with a low class of wind resource.



(a)



(b)

Figure 11. Cont.

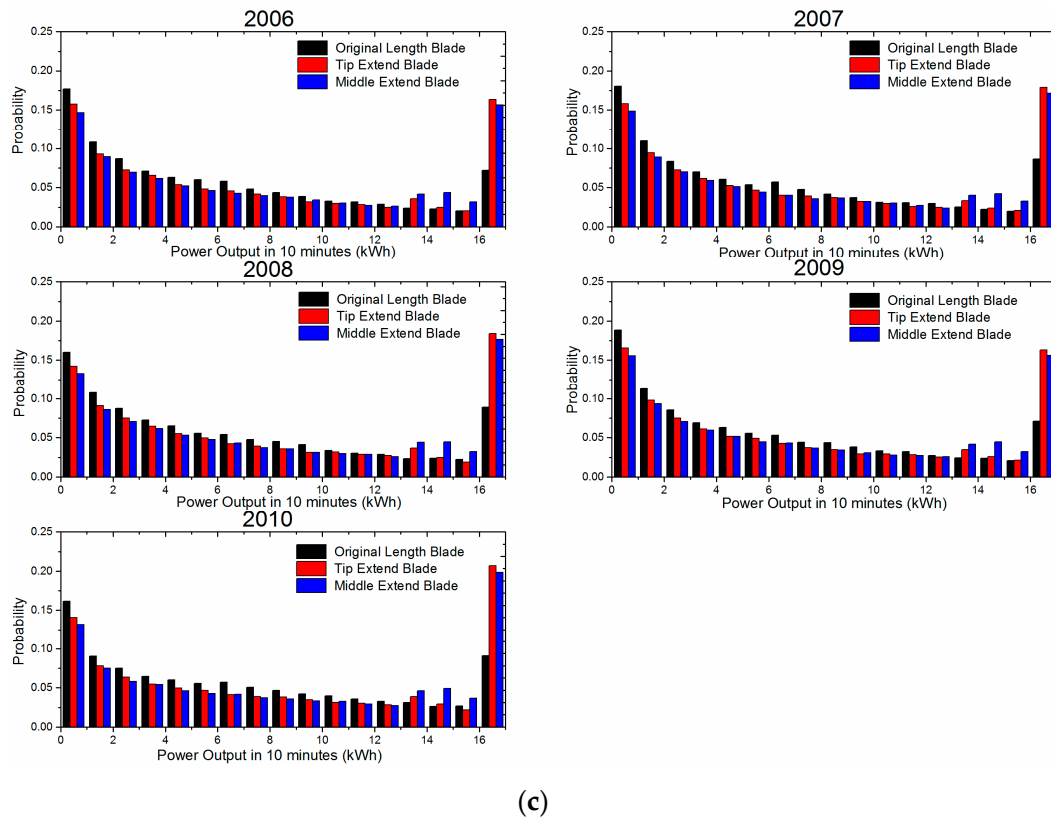


Figure 11. Statistical distribution of 10 min of energy output for the original blade and extensible blades at (a) Site A; (b) Site B; (c) Site C.

Table 6 summarizes the predicted total annual energy production by different types of blades (original versus extensible blades). The results show that the innovative extensible wind turbine blades will potentially increase the total annual wind energy production for all sites with a low class of wind. For Site A, the extensible blade that extends at the tip will increase the power output by around 19%; the extensible blade that extends in the middle will increase the power output by 32%. For Site B, the corresponding increases in total energy production are 22% and 31% by the two types of extensible blades. For Site C, the amount of increase in the annual energy production for tip extension and middle extension blades are around 19% and 25% respectively. The extensible blade that extends in the middle provides a larger increase in the energy output than that extends at the tip due to the larger wind carry areas; besides this, the percentage increase in energy production is more significant at site with a low class of wind (i.e., Sites A and B) than site with high class of the wind (i.e., Site C). These are a clear demonstration of the benefits of the extensible blade to boost energy production for a site with low classes of wind. In the meantime, the extension scheme is designed so that the extensible blade is protected with a similar structural safety to a regular blade.

Table 6. Comparison of total annual energy production by the original blade versus extensible blades at different sites.

Year	Energy Output by Original Blade (kWh)	Energy Output by Tip Extended Blade (kWh)	Increase Percentage (%)	Energy Output by Middle Extended Blade (kWh)	Increase Percentage (%)
Site A (Class 4, Onshore)					
2011	80,316.25	95,692.79	19.14	106,387.10	32.46
2012	73,393.83	87,562.00	19.30	97,316.17	32.59
2013	78,277.17	92,783.17	18.53	103,071.30	31.67
2014	75,296.00	89,820.17	19.29	99,600.17	32.28
Site B (Class 4, Onshore)					
2010	44,819.83	55,296.00	23.37	59,269.00	32.24
2011	70,515.67	85,525.50	21.29	92,656.17	31.40
2012	93,464.50	114,019.3	21.99	121,786.50	30.30
Site C (Class 3, Offshore)					
2006	308,698.30	368,768.30	19.46	387,289.30	25.46
2007	314,257.70	372,854.80	18.65	390,657.80	24.31
2008	322,774.70	382,870.50	18.62	401,353.30	24.34
2009	305,493.20	364,615.70	19.35	382,645.30	25.25
2010	239,212.20	284,880.20	19.09	297,576.30	24.40

6. Conclusions

Wind farms are ideally located at locations with high-class wind. However, there are a large number of distributed wind turbines constructed at sites close to communities, with non-ideal wind conditions. This paper describes the analyses of an innovative, extensible blade technology that aims to utilize wind energy in areas with low-class wind resources. The extensible blade functions by adjusting its length depending on the wind conditions (i.e., it will extend at low wind speed and retract at high wind speed). Based on the principle that the larger the sweep area, the higher the turbine energy output, dynamically adjusting the blade length helps to increase the energy output under low wind speed while mitigating safety risks under high wind speed. The computational model is developed based on the blade element momentum (BEM) theory, which determines the aerodynamic load and power output of the blade at different wind conditions. The model is firstly validated with monitored energy output data of in-service wind turbine. The validated model is subsequently used to estimate the annual energy production by the extensible blades and regular blade at three locations inland and offshore of the Lake Erie area, where yearly wind data are continuously monitored. Two types of extensible blade scheme are analyzed; i.e., extension in the middle of the blade versus extension at the tip of the blade. The extension and contraction scheme of these extensible blades are determined based on a limiting of the maximum bending moment acting on the blade, which helps ensure their structural safety. The influence of blade extension on the dynamic characteristics of blade structure is analyzed. The results show that the extensible blade will potentially increase annual energy output up to 20% to 30% for the sites analyzed. Besides this, the lower the wind speed, the more effective the extensible blade in increasing energy production. Overall, the results of this paper point to the promise of this innovative, extensible blade in improving the wind energy production.

Acknowledgments: This research is partially supported by the US National Science Foundation CMMI-1300149.

Author Contributions: Xiong (Bill) Yu conceived the concept of extensible blade and control criteria for blade extension. Jiale Li conducted the detailed modeling and analyses under the guidance to quantify the performance of extensible blade in improving energy production. Both authors contributed to the write up and refinement of this paper.

Conflicts of Interest: The authors declare no conflict of interest. The option raised by this paper does not represent the opinion of the sponsor.

Appendix A. Implementation Procedures of Beam Element Momentum (BEM) Theory for Turbine Energy Output Prediction

BEM is composed of two different theories, i.e., blade element theory and momentum theory [37]. Blade element theory assumes that blades can be divided into small elements that act independently of the surrounding elements and operate aerodynamically as two-dimensional airfoils as shown in Figure A1, in which α is the attack angle. The characteristics of blade responses (drag and lift on each element) are determined by the angle of attack of incoming wind, which is the angle between the center reference line of the geometry and the relative incoming flow W (Figure A1). The momentum theory assumes that the loss of air pressure or generation of turning momentum in the airfoil blade element is caused by the work done by the incoming airflow [38]. The BEM theory couples these two theories together and calculates the total lift and momentum via an iterative process [39].

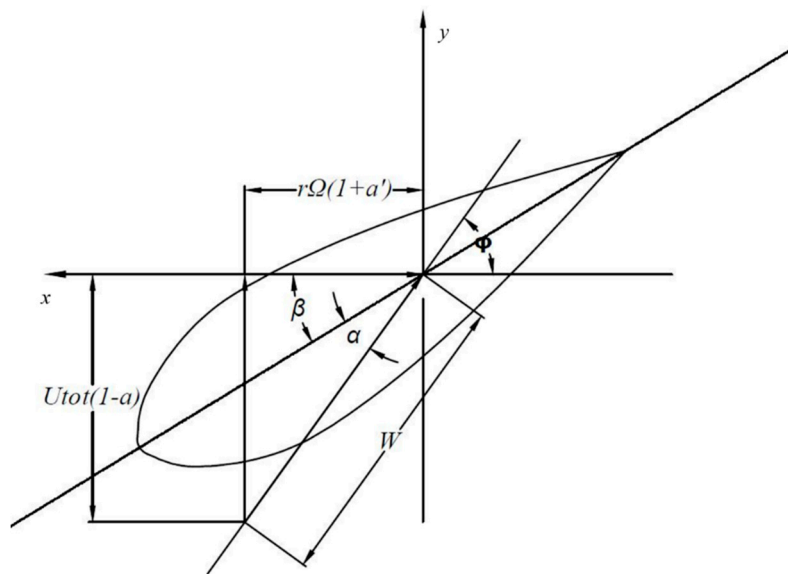


Figure A1. Blade Element velocity components.

Appendix A.1. Blade Element Momentum (BEM) Theory

The actual wind flow acting on the turbine rotor is rather complex and can be simplified by the use of the blade element theory. The velocity components in the radial positions of the blade can be expressed regarding the wind speed, the axial induction factor (a), tangential flow induction factors (a') and the rotational speed of the rotor (Ω). The axial flow induction factor (a) and the tangential flow induction factor (a') are critical parameters in the BEM theory. Figure A1 illustrates the conceptual model to calculate the lift and draft forces on each airfoil blade element. The airfoil is assumed to have a blade pitch angle of β , and the wind acts on the airfoil with an attack angle α . The pitch angle is the angle between the blade chord and normal direction of the rotor plane, which is an important parameter for maximizing blade lift and determines the load acting on the blade. The component of wind velocity in the direction of the blade is ignored as it does not contribute to the torque on the blade rotation. Therefore, the inflow angle ϕ which is the intersection angle between the inflow wind velocity and the rotation plane of the blades, satisfying the following relationship:

$$\phi = \alpha + \beta \quad (\text{A1})$$

BEM theory does not include the effects of tip losses, hub losses, skewed values, dynamic stall, and tower shadow. The lift and drag forces generated by the airfoil along the blade and the momentum equations are used to produce the induction factors. The calculation step was then organized into a series of equations that can be solved iteratively, which is further elaborated in the following sections.

Appendix A.2. The Calculation of Relative Inflow Wind Velocity

An important assumption of the blade element momentum (BEM) theory is that the lift and drag forces acting on a blade element are solely responsible for the momentum which caused by the air passing through the blade swept annulus [55]. Lift and draft forces are determined by the relative wind velocity act on the airfoil. The wind velocity perpendicular to the rotor plane is the inflow wind velocity $U_{\text{tot}}(t)$ reduced by the amount of $a \times U_{\text{tot}}(t)$ due to axial interference (i.e., $(1 - a) \times U_{\text{tot}}(t)$). Assuming the rotor rotates with angular speed Ω , the blade element at a distance r from the rotor axis will be moving with a tangential speed Ωr [56]. When the wind passes through the rotor plane and interacts with the moving rotor, a tangential slipstream (or wake rotation) of wind velocity $a' \Omega r$ is introduced. The resultant inflow wind velocity about the rotor blade W is shown in Figure A1 and can be calculated via the procedures are shown in the following:

$$W = \sqrt{U_{\text{tot}}^2(1 - a)^2 + [\Omega r(1 + a')]^2} \quad (\text{A2})$$

And the inflow angle φ could also express using the velocity:

$$\varphi = \arctan\left[\frac{U_{\text{tot}}(1 - a)}{\Omega r(1 + a')}\right] \quad (\text{A3})$$

To calculate the relative incoming wind speed, W at each position r along the length of the blade and for each total wind speed U_{tot} , the axial flow induction factor a and tangential flow induction factor a' need to be calculated first. Typically, this is done via an iterative numerical procedure, with the basic steps as follows [2,57,58]:

- Assume an initial choice of a and a' . (for example $a = a' = 0$ as an initial guess). Calculate the inflow angle via $\varphi = \arctan\left[\frac{U_{\text{tot}}(1 - a)}{\Omega r(1 + a')}\right]$, where Ω is the rotor angular speed.
- Calculate $\alpha = \varphi - \beta$;
- Read C_l and C_d from the lift and drag coefficient curves shown in Figure 3 with the result of α from step b. Calculate the coefficient of sectional blade element force normal to the rotor plane C_x and coefficient of sectional blade element force parallel to the rotor plane C_y :

$$C_x = C_l \times \cos \varphi + C_d \times \sin \varphi$$

$$C_y = C_l \times \sin \varphi + C_d \times \cos \varphi$$

- Substitute C_x and C_y into the following expressions to calculate new values for a and a'

$$\frac{a}{1 - a} = \frac{\sigma_r}{4 \times \sin^2 \varphi} \left(C_x - \frac{\sigma_r}{4 \sin^2 \varphi} C_y^2 \right)$$

$$\frac{a'}{1 + a'} = \frac{\sigma_r C_y}{4 \times \sin \varphi \cos \varphi}$$

$$\sigma_r = 3 \times \frac{C(r)}{2\pi r}$$

- Evaluate convergence of the solution by comparing the calculated a and a' from step e with the assumed a and a' from step a.

- f. If the differences between values are smaller than designated threshold, the process stops. Otherwise, update a and a' values and continue the iteration between (b) and (e) until the results converge.
- g. Take the result of a and a' into Equation (A2) to calculate the relative wind speed W .

The procedure shown above applies to different types of turbine blades. It also needs to note that as the lift and drag coefficients vary with attack angle, variable pitch wind turbine modulates the wind attack angle by dynamically adjust the pitch angle of blades.

Appendix A.3. Blade Lift and Drag Force Calculation

The relative wind velocity gives rise to aerodynamic lift and drag forces acting on each segment of the blade, which can be calculated as follows:

$$F_L(r) = \frac{1}{2} C_l \rho C(r) W^2 r \quad (\text{A4})$$

$$F_D(r) = \frac{1}{2} C_d \rho C(r) W^2 r \quad (\text{A5})$$

where $C(r)$ is blade chord length; r stands for the distance from the hub of a section of the blade; C_l is the lift coefficient, C_d is the drag coefficient.

The differential torque act on a blade section is

$$dT = r dF_T = F_L \sin \varphi - F_D \cos \varphi = \frac{1}{2} \rho W^2 C(r) C_y \quad (\text{A6})$$

The shaft power is calculated via total torque and rotor angular speed

$$P_m = T \Omega = \int_0^r dT \Omega \quad (\text{A7})$$

$$P_w = C_p P_m \quad (\text{A8})$$

where P_w is wind turbine production power, Ω is rotor speed; P_m is shaft power; C_p is the power coefficient.

In summary, the driving force on a wind turbine is generated by lift force when the wind flows past the airfoils. The lift force increases with attack angle, which is also accompanied by increases in undesirable drag force. While the tangential component of lift force supports blade rotation, drag force opposes it at the same time. Therefore, a wind turbine will achieve the best performance when the ratio of lift force to drag force is maximum, or at its optimum attack angle. Airfoil cross sections are aligned in a way to operate at close to optimum attack angle. The torque is dependent on the blade section chord length (C), and the relative inflow wind velocity W , which varies along the blade length. They are also dependent on the air density. The power output can be calculated by multiplying the rotational speed and the torque acting on blades. The procedure is also illustrated in Figure A2.

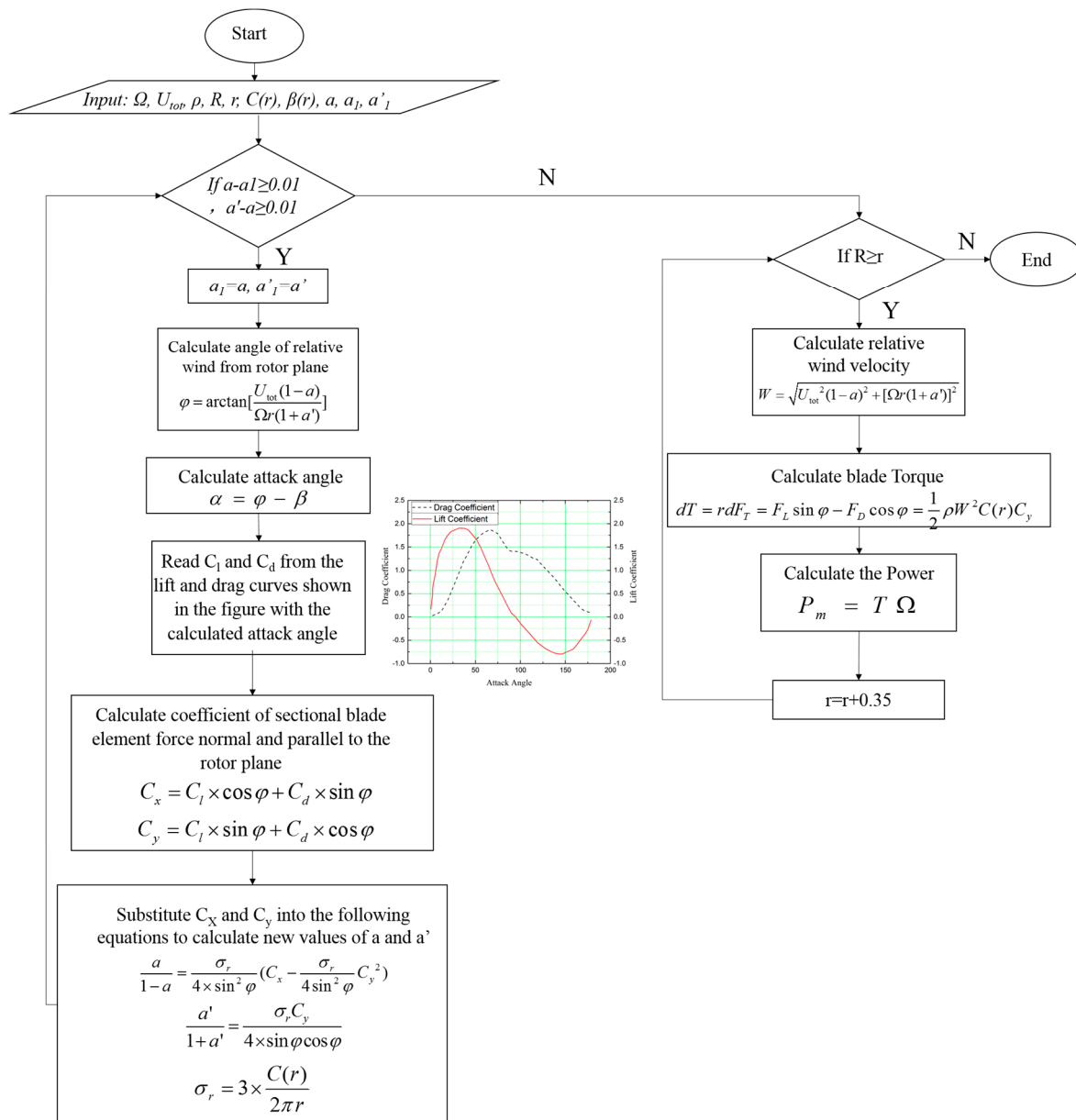


Figure A2. Flowchart for calculating blade production power using BEM theory.

References

1. Carlin, P.W.; Laxson, A.S.; Muljadi, E. The history and state of the art of variable-speed wind turbine technology. *Wind Energy* **2003**, *6*, 129–159. [\[CrossRef\]](#)
2. Burton, T.; Sharpe, D.; Jenkins, N.; Bossanyi, E. *Wind Energy Handbook*; John Wiley & Sons: Hoboken, NJ, USA, 2001.
3. IEC 61400-3: *Wind Turbines—Part 1: Design Requirements*; TC88-MT; International Electrotechnical Commission: Geneva, Switzerland, 2005.
4. Chen, K.; Song, M.; Zhang, X. The iteration method for tower height matching in wind farm design. *J. Wind Eng. Ind. Aerodyn.* **2014**, *132*, 37–48. [\[CrossRef\]](#)
5. Li, J.; Yu, X.B. LiDAR technology for wind energy potential assessment: Demonstration and validation at a site around Lake Erie. *Energy Convers. Manag.* **2017**, *144*, 252–261. [\[CrossRef\]](#)
6. Wang, X.; Yang, X.; Zeng, X. Centrifuge modeling of lateral bearing behavior of offshore wind turbine with suction bucket foundation in sand. *Ocean Eng.* **2017**, *139*, 140–151. [\[CrossRef\]](#)

7. Wang, X.; Yang, X.; Zeng, X. Seismic Centrifuge Modelling of Suction Bucket Foundation for Offshore Wind Turbine. *Renew. Energy* **2017**, in press. [[CrossRef](#)]
8. Calvert, S.; Thresher, R.; Hock, S.; Laxson, A.; Smith, B. US department of energy wind energy research program for low wind speed technology of the future. *J. Sol. Energy Eng.* **2002**, *124*, 455–458. [[CrossRef](#)]
9. Robinson, M.; Veers, P. US national laboratory research supporting low wind speed technology. *Trans. Am. Soc. Mech. Eng. J. Sol. Energy Eng.* **2002**, *124*, 458–459. [[CrossRef](#)]
10. Zhang, J.; Zhou, Z.; Lei, Y. Design and Research of High-Performance Low-Speed Wind Turbine Blades. In Proceedings of the World Non-Grid-Connected Wind Power and Energy Conference (WNWEC 2009), Nanjing, China, 24–26 September 2009; pp. 1–5.
11. Barnes, R.; Morozov, E.; Shankar, K. Improved methodology for design of low wind speed specific wind turbine blades. *Compos. Struct.* **2015**, *119*, 677–684. [[CrossRef](#)]
12. Wichser, C.; Klink, K. Low wind speed turbines and wind power potential in Minnesota, USA. *Renew. Energy* **2008**, *33*, 1749–1758. [[CrossRef](#)]
13. Alam, M.M.; Rehman, S.; Meyer, J.P.; Al-Hadhrami, L.M. Review of 600–2500 kW sized wind turbines and optimization of hub height for maximum wind energy yield realization. *Renew. Sustain. Energy Rev.* **2011**, *15*, 3839–3849. [[CrossRef](#)]
14. Lee, J.; Kim, D.R.; Lee, K.-S. Optimum hub height of a wind turbine for maximizing annual net profit. *Energy Convers. Manag.* **2015**, *100*, 90–96. [[CrossRef](#)]
15. Rehman, S.; Al-Hadhrami, L.M.; Alam, M.M.; Meyer, J.P. Empirical correlation between hub height and local wind shear exponent for different sizes of wind turbines. *Sustain. Energy Technol. Assess.* **2013**, *4*, 45–51. [[CrossRef](#)]
16. Pellegrino, A.; Meskell, C. Vortex shedding from a wind turbine blade section at high angles of attack. *J. Wind Eng. Ind. Aerodyn.* **2013**, *121*, 131–137. [[CrossRef](#)]
17. No, T.; Kim, J.-E.; Moon, J.; Kim, S. Modeling, control, and simulation of dual rotor wind turbine generator system. *Renew. Energy* **2009**, *34*, 2124–2132. [[CrossRef](#)]
18. Huang, G.-Y.; Shiah, Y.; Bai, C.-J.; Chong, W. Experimental study of the protuberance effect on the blade performance of a small horizontal axis wind turbine. *J. Wind Eng. Ind. Aerodyn.* **2015**, *147*, 202–211. [[CrossRef](#)]
19. Miklosovic, D.; Murray, M.; Howle, L.; Fish, F. Leading-edge tubercles delay stall on humpback whale (*Megaptera novaeangliae*) flippers. *Phys. Fluids* **2004**, *16*, L39–L42. [[CrossRef](#)]
20. Huang, D.; Wu, G. Preliminary study on the aerodynamic characteristics of an adaptive reconfigurable airfoil. *Aerosp. Sci. Technol.* **2013**, *27*, 44–48. [[CrossRef](#)]
21. Bhuyan, S.; Biswas, A. Investigations on self-starting and performance characteristics of simple H and hybrid H-Savonius vertical axis wind rotors. *Energy Convers. Manag.* **2014**, *87*, 859–867. [[CrossRef](#)]
22. Bottasso, C.L.; Croce, A.; Gualdoni, F.; Montinari, P. Load mitigation for wind turbines by a passive aeroelastic device. *J. Wind Eng. Ind. Aerodyn.* **2016**, *148*, 57–69. [[CrossRef](#)]
23. Veers, P.S.; Ashwill, T.D.; Sutherland, H.J.; Laird, D.L.; Lobitz, D.W.; Griffin, D.A.; Mandell, J.F.; Musial, W.D.; Jackson, K.; Zuteck, M. Trends in the design, manufacture and evaluation of wind turbine blades. *Wind Energy* **2003**, *6*, 245–259. [[CrossRef](#)]
24. Bir, G.S. Computerized method for preliminary structural design of composite wind turbine blades. *J. Sol. Energy Eng.* **2001**, *123*, 372–381. [[CrossRef](#)]
25. Jackson, K.; Zuteck, M.; Van Dam, C.; Standish, K.; Berry, D. Innovative design approaches for large wind turbine blades. *Wind Energy* **2005**, *8*, 141–171. [[CrossRef](#)]
26. Griffin, D.A. *Blade System Design Studies Volume I: Composite Technologies for Large Wind Turbine Blades*; Paper No. SAND-1879 2002; Sandia National Laboratories: Livermore, CA, USA, 2002.
27. Griffin, D.A. *WindPACT Turbine Design Scaling Studies Technical Area 1—Composite Blades for 80- to 120-m Rotor*; Technical Report; National Renewable Energy Laboratory: Livermore, CA, USA, 2001.
28. Jureczko, M.; Pawlak, M.; Mężyk, A. Optimisation of wind turbine blades. *J. Mater. Process. Technol.* **2005**, *167*, 463–471. [[CrossRef](#)]
29. Sharma, R.; Madawala, U. The concept of a smart wind turbine system. *Renew. Energy* **2012**, *39*, 403–410. [[CrossRef](#)]

30. Imraan, M.; Sharma, R.N.; Flay, R.G. Wind tunnel testing of a wind turbine with telescopic blades: The influence of blade extension. *Energy* **2013**, *53*, 22–32. [[CrossRef](#)]
31. McCoy, T.J.; Griffin, D.A. Control of rotor geometry and aerodynamics: Retractable blades and advanced concepts. *Wind Eng.* **2008**, *32*, 13–26. [[CrossRef](#)]
32. Singh, M.; Santoso, S. *Dynamic Models for Wind Turbines and Wind Power Plants*; National Renewable Energy Laboratory: Livermore, CA, USA, 2011.
33. Dai, J.; Liu, D.; Wen, L.; Long, X. Research on power coefficient of wind turbines based on SCADA data. *Renew. Energy* **2016**, *86*, 206–215. [[CrossRef](#)]
34. Li, J.; Yu, X. Model and Procedures for Reliable Near Term Wind Energy Production Forecast. *Wind Eng.* **2015**, *39*, 595–608. [[CrossRef](#)]
35. Jonkman, J.M.; Butterfield, S.; Musial, W.; Scott, G. *Definition of a 5-MW Reference Wind Turbine for Offshore System Development*; National Renewable Energy Laboratory: Livermore, CA, USA, 2009.
36. Glauert, H. Airplane propellers. In *Aerodynamic Theory*; Springer: New York, NY, USA, 1935; pp. 169–360.
37. Leishman, J. *Principles of Helicopter Aerodynamics*; Cambridge University Press: New York, NY, USA, 2000.
38. Moriarty, P.J.; Hansen, A.C. *AeroDyn Theory Manual*; National Renewable Energy Laboratory: Golden, CO, USA, 2005.
39. Kulunk, E. Aerodynamics of wind turbines. In *Fundamental and Advanced Topics in Wind Power*; InTech: Rijeka, Croatia, 1970.
40. Gorsevski, P.V.; Cathcart, S.C.; Mirzaei, G.; Jamali, M.M.; Ye, X.; Gomezdelcampo, E. A group-based spatial decision support system for wind farm site selection in Northwest Ohio. *Energy Policy* **2013**, *55*, 374–385. [[CrossRef](#)]
41. Mekonnen, A.D.; Gorsevski, P.V. A web-based participatory GIS (PGIS) for offshore wind farm suitability within Lake Erie, Ohio. *Renew. Sustain. Energy Rev.* **2015**, *41*, 162–177. [[CrossRef](#)]
42. Wang, X.; Yang, X.; Zeng, X. Lateral capacity assessment of offshore wind suction bucket foundation in clay via centrifuge modelling. *J. Renew. Sustain. Energy* **2017**, *9*, 033308. [[CrossRef](#)]
43. Klink, K. Atmospheric circulation effects on wind speed variability at turbine height. *J. Appl. Meteorol. Climatol.* **2007**, *46*, 445–456. [[CrossRef](#)]
44. Soler-Bientz, R. Preliminary results from a network of stations for wind resource assessment at North of Yucatan Peninsula. *Energy* **2011**, *36*, 538–548. [[CrossRef](#)]
45. Saleh, H.; Aly, A.A.E.-A.; Abdel-Hady, S. Assessment of different methods used to estimate Weibull distribution parameters for wind speed in Zafarana wind farm, Suez Gulf, Egypt. *Energy* **2012**, *44*, 710–719. [[CrossRef](#)]
46. Seguro, J.; Lambert, T. Modern estimation of the parameters of the Weibull wind speed distribution for wind energy analysis. *J. Wind Eng. Ind. Aerodyn.* **2000**, *85*, 75–84. [[CrossRef](#)]
47. Carta, J.A.; Ramirez, P.; Velazquez, S. A review of wind speed probability distributions used in wind energy analysis: Case studies in the Canary Islands. *Renew. Sustain. Energy Rev.* **2009**, *13*, 933–955. [[CrossRef](#)]
48. Foley, C.; Fournelle, R.; Ginal, S.J.; Peronto, J.L. *Structural Analysis of Sign Bridge Structures and Luminaire Supports*; Northwestern University: Evanston, IL, USA, 2004.
49. Durst, C. Wind speeds over short periods of time. *Meteorol. Mag.* **1960**, *89*, 181–186.
50. Holmes, J.D. *Wind Loading of Structures*; CRC Press: Boca Raton, FL, USA, 2015.
51. Pourazarm, P.; Caracoglia, L.; Lackner, M.; Modarres-Sadeghi, Y. Stochastic analysis of flow-induced dynamic instabilities of wind turbine blades. *J. Wind Eng. Ind. Aerodyn.* **2015**, *137*, 37–45. [[CrossRef](#)]
52. Chaudhari, N. Dynamic Characteristics of Wind Turbine Blade. *Int. J. Eng. Res. Technol.* **2014**, *8*.
53. Yanbin, C.; Lei, S.; Feng, Z. Modal Analysis of Wind Turbine Blade Made of Composite laminated plates. In Proceedings of the 2010 Asia-Pacific Power and Energy Engineering Conference (APPEEC), Chengdu, China, 28–31 March 2010; pp. 1–4.
54. Taslimi-Renani, E.; Modiri-Delshad, M.; Elias, M.F.M.; Rahim, N.A. Development of an enhanced parametric model for wind turbine power curve. *Appl. Energy* **2016**, *177*, 544–552. [[CrossRef](#)]

55. Det Norske Veritas and Riso National Laboratory. *Guidelines for Design of Wind Turbines*, 2nd ed.; DNV: Oslo, Norway, 2002.
56. Sedaghat, A.; Assad, M.E.H.; Gaith, M. Aerodynamics performance of continuously variable speed horizontal axis wind turbine with optimal blades. *Energy* **2014**, *77*, 752–759. [[CrossRef](#)]
57. Tenguria, N.; Mittal, N.; Ahmed, S. Investigation of blade performance of horizontal axis wind turbine based on blade element momentum theory (BEMT) using NACA airfoils. *Int. J. Eng. Sci. Technol.* **2010**, *2*, 25–35. [[CrossRef](#)]
58. Kulunk, E. *Aerodynamics of Wind Turbines, Fundamental and Advanced Topics in Wind Power*; Rupp, C., Ed.; InTech: Rijeka, Croatia, 2011; ISBN 978-953-307-508-2.



© 2017 by the authors. Licensee MDPI, Basel, Switzerland. This article is an open access article distributed under the terms and conditions of the Creative Commons Attribution (CC BY) license (<http://creativecommons.org/licenses/by/4.0/>).